Autophagy 10:2, 285–295; February 2014; © 2014 Landes Bioscience

Interorganelle interactions and inheritance patterns of nuclei and vacuoles in budding yeast meiosis

I-Ting Tsai,[1,2] Jyun-Liang Lin,[2] Yi-Hsuan Chiang,[1,2] Yu-Chien Chuang,[2,3] Shu-Shan Liang,[2,4] Chi-Ning Chuang,[2] Tzyy-Nan Huang,[2] and Ting-Fang Wang[1,2,3,4,*]

[1]Department of Life Sciences and Institute of Genome Sciences; National Yang-Ming University; Taipei, Taiwan; [2]Institute of Molecular Biology; Academia Sinica; Taipei, Taiwan; [3]Taiwan International Graduate Program in Molecular and Cellular Biology; Academia Sinica; Taipei, Taiwan; [4]Institute of Biochemical Sciences; National Taiwan University; Taipei, Taiwan

Keywords: meiosis, vacuoles, nucleus-vacuole junction, piecemeal microautophagy of the nucleus, nuclear envelope, bouquet formation, rapid prophase movements

Abbreviations: CFP, cyan fluorescent protein; GFP, green fluorescent protein; MI, first nuclear division; MII, second nuclear division; NE, nuclear envelope; NPC, nuclear pore complex; NVC, nucleus-vacuole contact; NVJ, nucleus-vacuole junction; PMN, piecemeal microautophagy of the nucleus; RPM, rapid prophase movement; SPB, spindle pole body; SPM, sporulation medium; tdm2, tdimer 2; TEM, transmission electron microscopy; V-ATPase, vacuolar proton-ATPase; YFP, yellow fluorescent protein; YPA, acetate-based medium

Many of the mechanisms by which organelles are inherited by spores during meiosis are not well understood. Dramatic chromosome motion and bouquet formation are evolutionarily conserved characteristics of meiotic chromosomes. The budding yeast bouquet genes (*NDJ1*, *MPS3*, *CSM4*) mediate these movements via telomere attachment to the nuclear envelope (NE). Here, we report that during meiosis the NE is in direct contact with vacuoles via nucleus-vacuole junctions (NVJs). We show that in meiosis NVJs are assembled through the interaction of the outer NE-protein Nvj1 and the vacuolar membrane protein Vac8. Notably, NVJs function as diffusion barriers that exclude the nuclear pore complexes, the bouquet protein Mps3 and NE-tethered telomeres from the outer nuclear membrane and nuclear ER, resulting in distorted NEs during early meiosis. An increase in NVJ area resulting from Nvj1-GFP overexpression produced a moderate bouquet mutant-like phenotype in wild-type cells. NVJs, as the vacuolar contact sites of the nucleus, were found to undergo scission alongside the NE during meiotic nuclear division. The zygotic NE and NVJs were partly segregated into 4 spores. Lastly, new NVJs were also revealed to be synthesized de novo to rejoin the zygotic NE with the newly synthesized vacuoles in the mature spores. In conclusion, our results revealed that budding yeast nuclei and vacuoles exhibit dynamic interorganelle interactions and different inheritance patterns in meiosis, and also suggested that *nvj1*△ mutant cells may be useful to resolve the technical challenges pertaining to the isolation of intact nuclei for the biochemical study of meiotic nuclear proteins.

Introduction

Meiosis is critical for sexual reproduction as it reduces the chromosomal complement to haploidy in preparation for fertilization. Haploidization is achieved by a single round of premeiotic DNA replication followed by various interactions (pairing, recombination, and synapsis) between homologous chromosomes during meiotic prophase. An important feature of meiosis in many organisms is that meiotic chromosomes undergo rapid prophase movements (RPMs).[1-12] These chromosomal movements are mediated by nuclear envelope attachment, the clustering of telomeres or centromeres, and physical linkage to the cytoskeleton in the cytosol. The meiosis-specific telomere clustering on the NE defines the bouquet stage, so named for its resemblance to the stems from a bouquet of cut flowers.[10,13]

In the budding yeast *Saccharomyces cerevisiae*, several bouquet proteins mediate RPMs and bouquet formation, including the meiosis-specific telomere-associated protein Ndj1/Tam1,[14-16] the essential spindle pole body (SPB) component Mps3,[17] and the tail-anchored endoplasmic reticulum (ER), and the outer nuclear membrane (ONM) protein Csm4.[18,19] Mps3 is localized to the SPB before the onset of premeiotic S-phase and then re-localizes into the inner nuclear membrane (INM) to mediate telomere-NE attachment during mid-prophase.[4,5,7,8] Csm4 was originally identified as a critical protein for accurate chromosome segregation

*Correspondence to: Ting-Fang Wang; Email: tfwang@gate.sinica.edu.tw
Submitted: 06/12/2013; Revised: 11/06/2013; Accepted: 11/13/2013
http://dx.doi.org/10.4161/auto.27192

during meiosis.[8,20] Together, Csm4 and Mps3 link telomeres to cytosolic actin bundles.[5,7,8] It is also notable that the budding yeast NE is "flattened" along one side during meiotic prophase.[7,9]

The vacuole is the most prominent organelle in the cytoplasm of the budding yeast *S. cerevisiae*. It is also the final destination of cytoplasmic proteins and organelles delivered via macroautophagy. These proteins or organelles are then degraded by vacuolar proteases. The vacuole is also subjected to "piecemeal microautophagy of the nucleus" (PMN), which degrades and recycles portions of the nucleus without killing the cell. PMN occurs at nucleus-vacuole junctions.[21] NVJs are formed through specific interactions between the ONM/ER protein Nvj1 and the vacuolar membrane protein Vac8, particularly during starvation.[21] Vac8 also has additional roles in protein targeting from the cytoplasm to the vacuole and in vacuole inheritance.[22] NVJs function as diffusion barriers to exclude the nuclear pore complex (NPC)[23-25] and the vacuolar proton-ATPase (V-ATPase).[26]

Progress in biochemical studies on budding yeast meiosis has been significantly impeded due to the high levels of vacuolar protease activity in the sporulating cells.[27,28] These vacuolar proteases (e.g., Pep4, Prb1, and Prc1) are highly induced upon starvation and are essential for sporulation.[29] Furthermore, it is technically difficult to exclude vacuoles in efforts to isolate intact meiotic nuclei.

Here, we applied genetic and live-cell imaging analyses to reveal the behavior and functional impact of NVJs on the NE and vacuoles throughout sporulation. We report that in meiosis the NE is in direct contact with vacuoles via the NVJs. We showed that NVJs are assembled through the interaction of the outer NE-protein Nvj1 and the vacuolar membrane protein Vac8 in meiosis. NVJs underwent scission alongside the NE during meiotic nuclear division, and a portion of the zygotic NE and NVJs were segregated into the 4 mature spores. We further suggest that the presence of NVJs in meiotic cells can (at least partly) account for the technical difficulties encountered in isolating intact meiotic nuclei, and therefore *nvj1*Δ mutant cells whose nuclei are not physically associated with the vacuoles, may be useful for the future biochemical study of meiotic nuclear proteins.

Results

Occurrence of NVJ during meiosis and sporulation

We performed live-cell imaging analyses to visualize NVJs, the NE and vacuoles with Nvj1-GFP, Nup49-tidmer2 (tdm2), and Vma2-tdm2 using a DeltaVision high-resolution fluorescence microscope (**Fig. 1**). Vma2 is a component of the 8-subunit V1 peripheral membrane domain of V-ATPase[30] Nup49 is an essential NPC subunit that is often used to mark the NE, and tdm2 is a monomeric variant of the red fluorescent protein DsRed.[31] GFP fused to Zip1, a meiosis-specific structural component of the synaptonemal complex,[32] was used to monitor meiotic cells at early- and mid-prophase.[7] The addition of tdm2 or GFP to these yeast proteins did not result in any apparent defect in sporulation efficiency, spore viability, or meiotic progression (data not shown). All GFP and tdm2 fusion proteins described here were expressed from their native promoters at their normal chromosomal locations. An amphiphilic fluorescent dye, FM 4–64, was also applied here to visualize vacuolar membranes in live meiotic cells that expressed Zip1-GFP, Nvj1-GFP, and Nup49-tdm2 (**Fig. S1**).

The heterozygous zygotes *NVJ1-GFP*/*NVJ1*, *ZIP1-GFP*/*ZIP1*, *NUP49-TDM2*/*NUP49*, and *VMA2-TDM2*/*VMA2* were incubated in a rich acetate-based medium (YPA) to temporarily arrest them in G_1 phase and were then transferred into sporulation medium (SPM) at 0 h to induce relatively synchronous meiosis. We found that the Nvj1-GFP patch appeared at the NVJs in G_1 (t = 0 h; **Fig. 1A**) and during meiotic prophase (t = 4 h; **Fig. 1B**). Notably, all the cells with Zip1-GFP also displayed Nvj1-GFP, indicating that NVJs indeed exist during meiotic prophase. Similar results were found in live meiotic prophase cells *NVJ1-GFP*/*NVJ1*, *ZIP1-GFP*/*ZIP1*, *NUP49-TDM2*/*NUP49*, and *VMA2*/*VMA2* stained with the vital dye FM4–64 (**Fig. S1**) except that only vacuolar membranes (**Fig. S1**) but not Vma2-tdm2 (**Fig. 1A and B**) were present in the NVJs.

Next, 2 Nvj1-GFP patches with nearly identical fluorescent intensities were detected at NVJs in cells undergoing their first nuclear division (MI) (**Fig. 1C**), suggesting that NVJs might undergo scission alongside the NE during MI. The Nvj1-GFP signals gradually diminished during the second nuclear division (MII) (**Fig. 1D**). Lastly, after the completion of sporulation, the tetrads of these heterozygous zygotes contained 2 mature spores with 1 prominent Nvj1-GFP patch each, whereas the other 2 spores showed 1 much weaker Nvj1-GFP patch each (t = 8 h; **Fig. 1E**). In contrast, the tetrads of the homozygous zygote *NVJ1-GFP*/*NVJ1-GFP* displayed 1 strong prominent NVJ1-GFP patch per spore (see below). These results suggest that new Nvj1-GFP proteins were also synthesized de novo in the *NVJ1-GFP* spores after MII (**Fig. 1D**) or during spore maturation (**Fig. 1E**).

We then performed quantitative imaging analysis to compare the relative Nvj1-GFP fluorescent intensity in the 4 mature spores of homozygous *NVJ1-GFP*/*NVJ1-GFP* tetrads and heterozygous *NVJ1-GFP*/*NVJ1* tetrads (**Fig. 2**). For each tetrad, the mature spore with the strongest Nvj1-GFP fluorescent signal was set to "1" as an internal fluorescent intensity reference. The relative average Nvj1-GFP fluorescent intensity of the other 3 spores in *NVJ1-GFP*/*NVJ1-GFP* homozygous tetrads (n = 20) was 0.86 ± 0.02, 0.74 ± 0.03 and 0.62 ± 0.03, respectively. In contrast, the relative average of Nvj1-GFP fluorescent intensity in the 20 heterozygous *NVJ1-GFP*/*NVJ1* tetrads (n = 20) was 0.80 ± 0.03, 0.32 ± 0.04, and 0.29 ± 0.02, respectively. Thus, in each mature spore, one-third to one-half of the Nvj1 directly derives directly from the zygote.

We also visualized 2 SPB components (Mps3-GFP and Spc29-CFP) along with Nup49-tdm2 and Vma2-tdm2 using the heterozygous zygotes *MPS3-GFP*/*MPS3*, *SPC29-YFP*/*SPC29*, *NUP49-TDM2*/*NUP49*, and *VMA2-TDM2*/*VMA2*. Mps3-GFP and Spc29-CFP were also expressed from their native promoters at their normal chromosomal locations. Mps3-GFP and Spc29-CFP colocalized at the SPB in G_1 phase (t = 0 h; **Fig. 1F**). During meiotic prophase, Mps3-GFP relocalized to the NE, whereas Spc29-CFP was retained at the SPB (t = 4 h; **Fig. 1G**). Immediately before MI, the SPB underwent duplication and

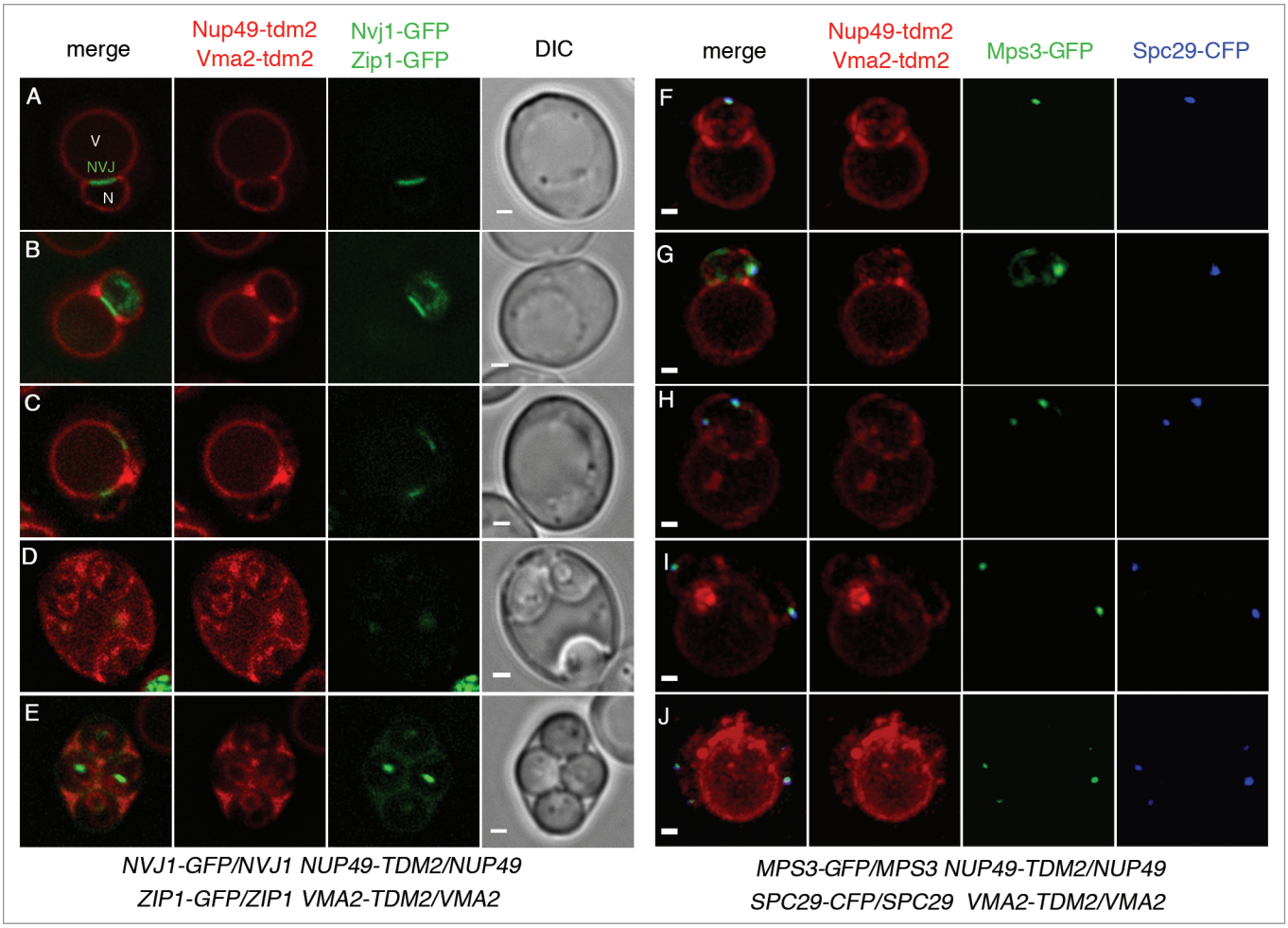

Figure 1. The vacuole is in contact with the NE via NVJs during meiosis and sporulation. Live-cell imaging analysis of the heterozygous zygotes *NVJ1/NVJ1-GFP*, *ZIP1-GFP/ZIP1*, *NUP49-TDM2/NUP49*, and *VMA2-TDM2/VMA2* (**A–E**) and the heterozygous zygotes *MPS3-GFP/MPS3*, *SPC29-CFP/SPC29*, *NUP49-TDM2/NUP49*, and *VMA2-TDM2/VMA2* (**F–J**) at indicated sporulation time points. Z-section images were captured of 27 slices spaced at 0.3 μm; a GFP image was taken every 0.3 s. mCherry was taken every 0.8 s. Single and stacked Z-section images are shown. N, nucleus; V, vacuole; NVJ: nucleus-vacuole junction. For 3D reconstruction, Z-section images were captured of 35 slices spaced at 0.2 μm. Mps3-YFP was taken every 1.5 s by GFP filter. Mps3-GFP was taken every 1.5 s by CFP filter. Nup49-tdimer and Vma2-tdimer were taken in 0.5 s by mCherry filter. Scale bar: 1 μm.

Mps3-GFP was localized to the 2 newly formed SPBs (t = 5 h; **Fig. 1H**). After MI, the 2 newly formed nuclei moved in the opposite directions on the exterior of the vacuole (t = 6 h; **Fig. 1I**). Lastly, at MII, the 2 nuclei and the 2 SPBs proceeded to undergo an additional round of duplication at the opposite poles of the vacuole, respectively (t = 6 h; **Fig. 1J**).

NVJ behavior during meiotic nuclear division and sporulation

We next applied the CellASIC ONIX microfluidic plates that were optimized for time-lapse live-cell imaging analysis to visualize NVJs after the heterozygous zygotes (*NVJ1-GFP*/*NVJ1* and *NUP49-TDM2*/*NUP49*) were incubated in SPM for 5 h. A stack of z-section images that covered the entire depth of the cell was assembled every 15 min. All z-section images at each time point were stacked and are presented side-by-side in **Figure 3** and **Figure S2**. The Nvj1-GFP patches indeed underwent scission during MI (t = 6.5–7 h) and MII (t = 9.5–11 h). In addition, the Nvj1-GFP patches that colocalized with the Nup49-tdm2 signals gradually diminished during the MI-MII transition. Meanwhile, the Nvj1-GFP signals also scattered in the zygote interior (t = 11.5 h).

There was some concern about the Nup49-tdm2 signals observed here, because it was previously reported that chromosomes are not surrounded by the NE during telophase II or in mature spores.[33] To clarify this point, we performed additional live-cell imaging experiments. The results from these additional experiments differed from those of the previous report.[33] First, the chromosomes (visualized by DAPI staining) at telophase II were surrounded by Nup49-tdm2 and/or Nvj1-GFP, and Nup49-tdm2 and Nvj1-GFP were also detected in the lumenal spaces (**Fig. 4**). Second, Nup49-tdm2 showed an even distribution throughout the 4 mature spores of the heterozygous zygotes (*NUP49-TDM2*/*NUP49* and *FOB1-GFP*/*FOB1-GFP*) (**Fig. 5A**). Fob1 is a nucleolar protein that is required for the programmed replication fork block in the rDNA.[34] We also showed that Nup49-tdm2 and Nup49-GFP were evenly distributed throughout the 4 mature spores of the heterozygous

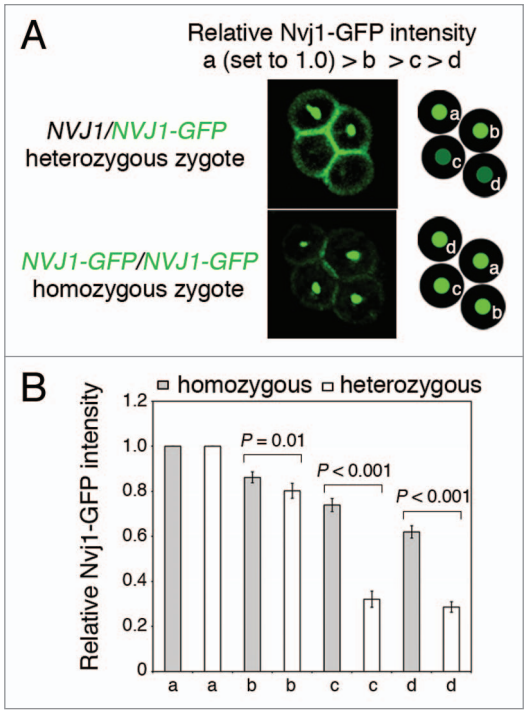

Figure 2. A portion of Nvj1 in the mature spores is directly derived from the zygotes. (**A**) Strategy used for quantitative analysis of the relative Nvj1-GFP fluorescent intensity in all 4 mature spores (a–d). The order of Nvj1-GFP fluorescent intensity was a > b > c > d, and the fluorescent intensity of the spore "a" was set to 1. (**B**) Relative Nvj1-GFP fluorescent intensity of all 4 mature spores. The data represent mean values ± SEM (error bars). n = 20.

zygote *NUP49-TDM2/NUP49-GFP* (**Fig. 5B**). Contrary to the previous report,[33] our data indicate that the NE was not only eliminated (in part) into the ascus lumen but was also segregated evenly into the 4 spores. These discrepancies are likely due to the use of a different cytology method for monitoring NPCs and the NE in the earlier report, i.e., by immunostaining of the fixed meiotic cells with an antibody against Nsp1, a NPC component.[33] We inferred that the NPC became inaccessible to the anti-Nsp1 antibody during or after MII due to the presence of prospore membranes over the nuclear surfaces. Consistent with this hypothesis, it was previously reported that the closure of the prospore membranes begins at anaphase II (or before telophase II) and is completed in the mature spores.[35,36]

Because NVJs are the vacuolar contact sites of the NE, we next monitored Vma2-tdm2 and the vacuolar protease Pep4-YFP in the mature tetrads by live-cell imaging. We found that in the tetrads of *PEP4-YFP/PEP4-YFP* homozygous zygotes, Nup49-tdm2, Pep4-YFP, and Vma2-tdm2 filled the entire lumen of the ascus (**Fig. S3**). In addition, Pep4-YFP was enclosed inside the vacuoles (Vma2-tdm2) of the mature spores (**Fig. S3A and S3B**). Moreover, the NE (Nup49-tdm2) was in close contact with the vacuole (Pep4-YFP) (**Fig. S3C**). In contrast, in the tetrads of *PEP4-YFP/PEP4 VMA2-TDM2/VMA2-TDM2* heterozygous zygotes, Pep4-YFP existed not only in the ascus lumen but also exclusively in the vacuoles of 2 (not 4) mature spores (**Fig. S3B**). These results are consistent with previous reports that zygotic vacuolar materials are discharged into the ascus lumen and that new vacuolar materials are regenerated inside the spores during spore maturation.[37,38]

Notably, in the tetrads of *NVJ1-GFP/NVJ1 VMA2-TDM2/VMA2* heterozygous zygotes, all 4 spores displayed Vma2-tdm2

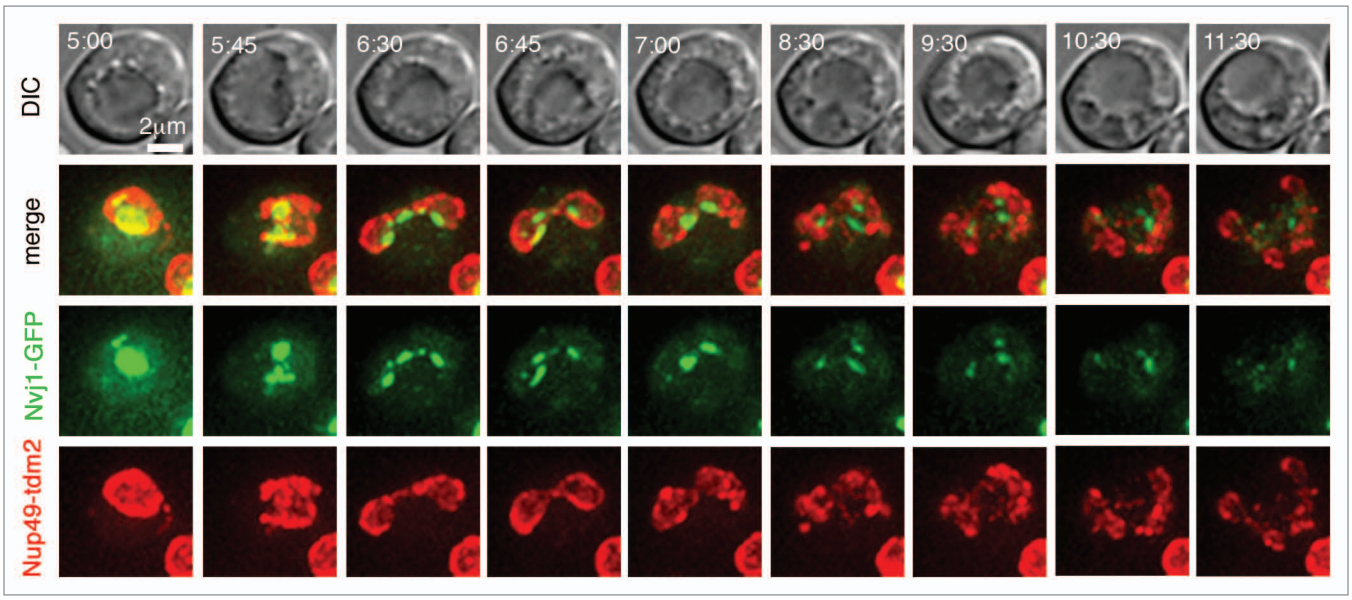

Figure 3. Time-lapse, live-cell imaging of Nvj1-GFP and Nup49-tdm2 from mid-prophase to MII. The *NVJ1-GFP/NVJ1*, *NUP49-TDM2/NUP49* heterozygous zygotes were transferred into SPM for 5 h, and then applied to a CellASIC ONIX microfluidic plate for time-lapsed live-cell imaging. For time-lapse imaging analyses of single, equatorial planes, Z-section images were captured of 18 slices spaced at 0.4 μm; a GFP image was taken every 0.25 s. mCherry was taken every 0.3 s. All z-section images at each time point were stacked and presented. Scale bar: 2 μm. Representative images at 5 h, 5¾ h, 6½ h, 6¾ h, 7 h, 8½ h, and 9 h time points are shown. All 18 images are shown in **Figure S2**.

signals (**Fig. S4A**). Thus, the Vma2-tdm2 proteins of the 2 *VMA2* spores apparently came from the zygotic vacuoles. The zygotic Vma2-tdm2 likely segregated alongside the NE and chromosomes and was then enclosed by the prospore membranes after MII.[35,36] In contrast, in the tetrads of *NVJ1-GFP*/*NVJ1 NUP49-TDM2*/*NUP49* heterozygous zygotes, Nvj1-GFP existed in all 4 mature spores but the GFP signals were much stronger in 2 of the 4 spores (**Fig. S4B**).

In summary, our results indicated that the majority of the zygotic NE, NVJs, and vacuolar materials are discharged into spore lumens. However, a portion of the zygotic NE, NVJs, and vacuolar membranes is retained and segregated alongside the chromosomes into the 4 mature spores. After the completion of prospore membrane closure and/or during spore maturation, new Nvj1 proteins and vacuolar materials (e.g., Pep4) were also synthesized de novo.

Nvj1 and Vac8 mediate the formation of NVJs in meiotic cells

The ONM/ER protein Nvj1 and the vacuolar membrane protein Vac8 form NVJs in haploid vegetative cells, particularly during starvation.[21] We therefore next examined the genetic requirement of NVJs during meiosis. Thin-section transmission electron microscopy (TEM) was applied to visualize the nuclei and vacuoles in P_{MCD1}-*cdc5* (**Fig. S5A–S5D**), wild-type (**Fig. S5E–S5G**), *nvj1*Δ (**Fig. S5H and S5I**) and *vac8*Δ (**Fig. S5J and S5K**) zygotes. Ninety to 100 thin serial sections (each 75 nm in thickness) were cut and negatively stained. P_{MCD1}-*cdc5* is a diploid mutant whose sole *CDC5* polo-like kinase gene is under the control of the *MCD1* promoter. The P_{MCD1}-*cdc5* mutant displays a classical pachytene arrest phenotype.[39] In the presence of Vac8 and Nvj1, 3 layers of membrane (INM, ONM, and vacuole membrane) were found at the NVJs (**Fig. S5A–S5G**; white

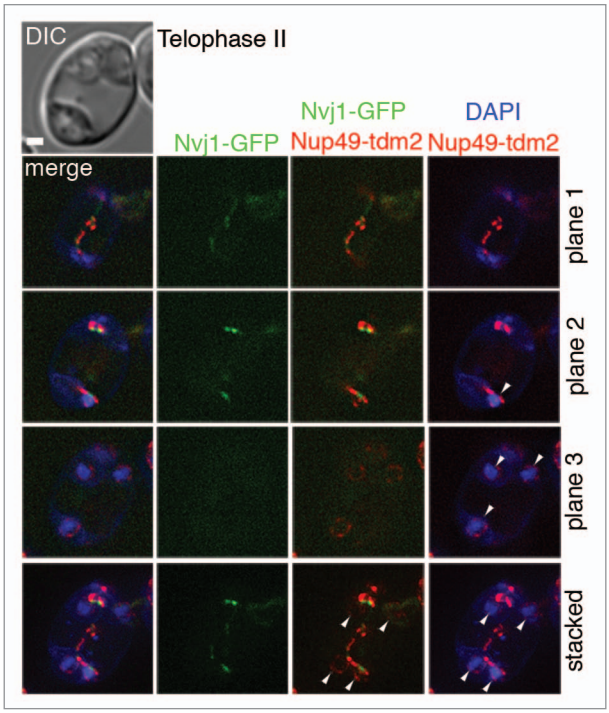

Figure 4. Distribution of chromosomes (DAPI), NVJs (Nvj1-GFP), and NPC (Nup49-tdm2) at telophase II. Live-cell imaging of the DAPI-stained *NVJ1-GFP*/*NVJ1*, *NUP49-TDM2*/*NUP49* heterozygous zygote. The cell was visualized by differential interference contrast (DIC) microscopy (top left panel). Z-section images were captured of 33 slices spaced at 0.3 μm; an FITC image was taken every 1 s. TRITC was taken every 1 s. DAPI was taken every 0.05 s. Three representative Z-sections images (plane 1–3) and stacked Z-section images (bottom panel) are shown. The 4 nuclei are indicated with white arrows. Scale bar: 1 μm.

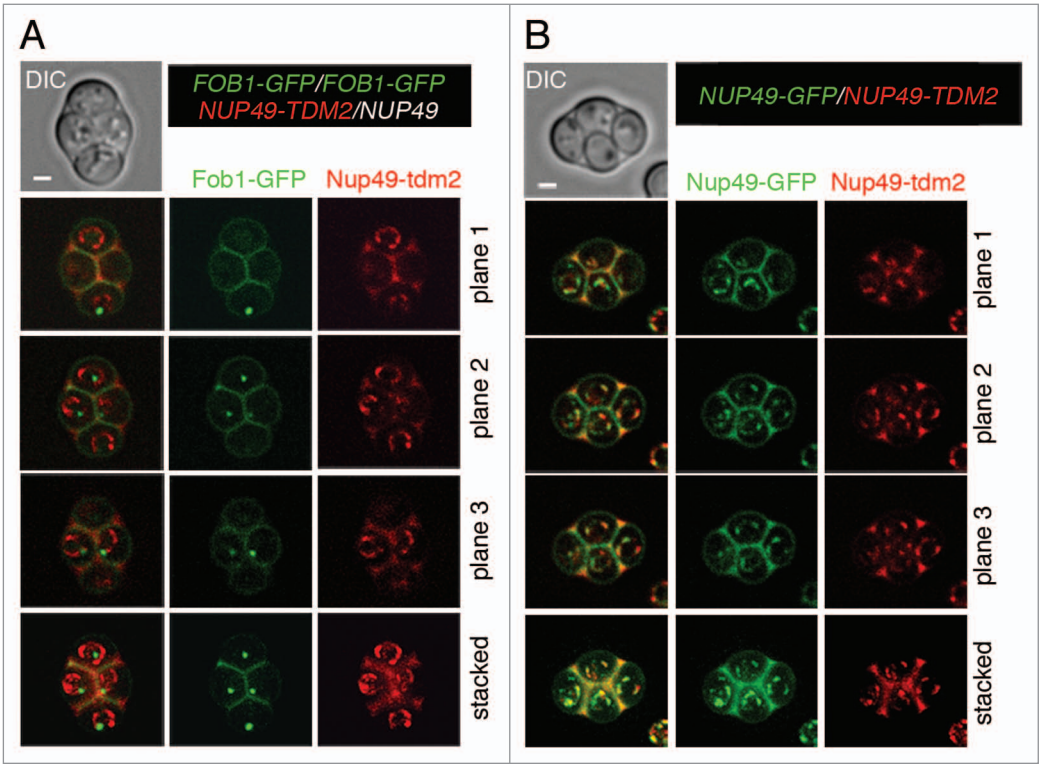

Figure 5. Distribution of Fob1-GFP, Nup49-tdm2, and Nup49-tdm2 in the mature tetrads of indicated zygotes. The mature spores were visualized by DIC microscopy (top-left panel). Z-section images were captured of 24 slices spaced at 0.3 μm; a GFP image was taken every 0.6 s. mCherry was taken every 0.3 s. Three representative Z-sections (i.e., plane 1–3) and stacked Z-section images (bottom panel) are shown. Scale bar: 1 μm.

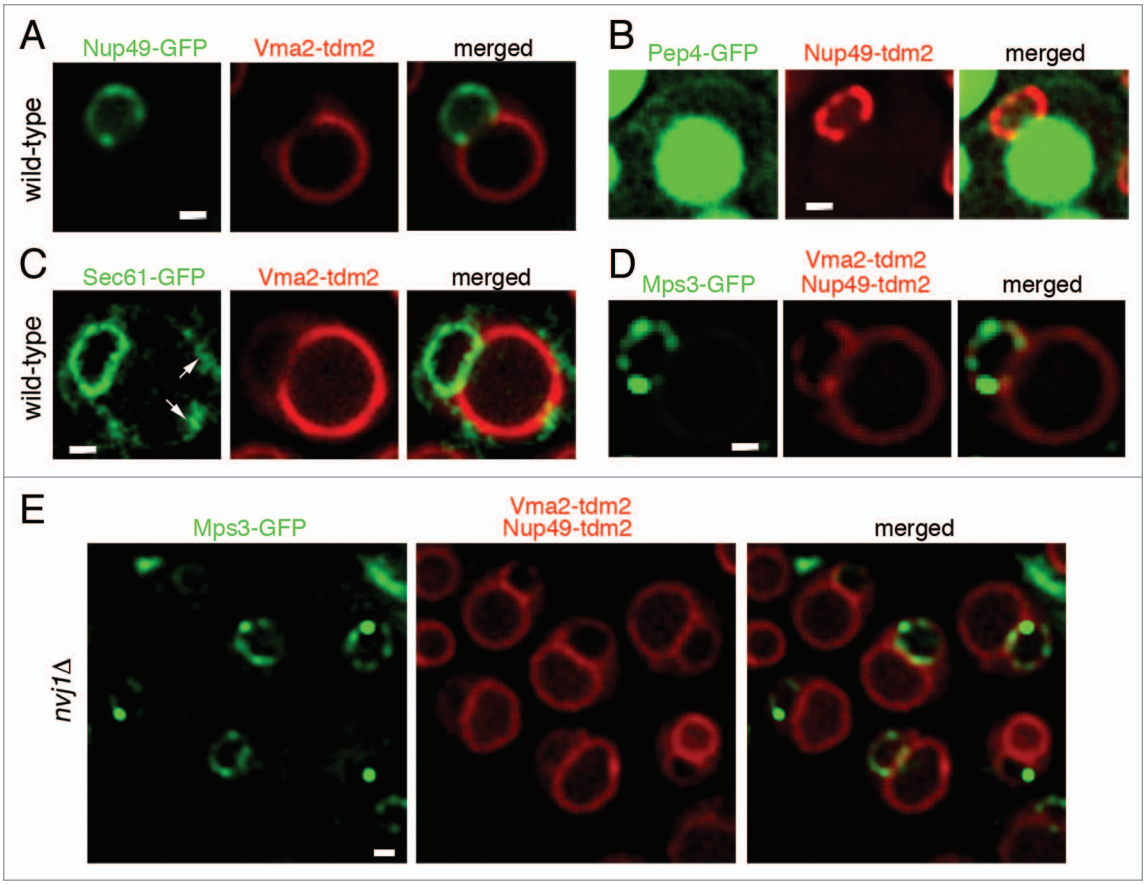

Figure 6. NVJs exclude NPC, V-ATPase, and Mps3 during meiosis. (**A and B**) Nup49-GFP, Vma2-tdm2, and Nup49-tdm2 are excluded from NVCs. (**C**) Sec61-GFP can be seen in the nuclear ER (including the NVC) and the cortical ER (indicated with white arrows). (**D**) In wild-type cells, Mps3-GFP appears as patches in the nuclear envelope but is excluded from NVJs. (**E**) In *nvj1*Δ zygotes, Mps3-GFP could be seen over the entire nuclear envelope (including NVC). For time-lapse imaging analyses of single, equatorial planes, 1 color image was taken every 0.33 s. For 3D reconstruction, Z-section images were captured of 30 slices spaced at 0.2 μm, or 14 slices at 0.6 μm in 1 s. Scale bar: 1 μm.

arrows), whereas only the INM and the ONM were observed in the non-NVJ regions of the NE (**Fig. S5A–S5G**; yellow arrows). In contrast, the NE was not in direct contact with the vacuoles in the *nvj1*Δ zygote (**Fig. S5H and S5I**) or the *vac8*Δ zygote (**Fig. S5J and S5K**) during meiosis. Accordingly, to mark the distinction, in *nvj1*Δ and *vac8*Δ, the contact sites between the nucleus and vacuoles visualized by fluorescence microscopy are referred to as the nucleus-vacuole contacts (NVCs) rather than NVJs.

As was previously reported for *vac8*Δ haploid cells under starvation conditions,[23] we also found that Nvj1-GFP failed to concentrate at the NVCs but, instead, encircled the entire NE of the *vac8*Δ zygotes (**Fig. S6**, top panels). Together, our results indicate that Nvj1 and Vac8 mediate the formation of NVJs during meiosis. In contrast, Nvj1-GFP was recruited into the NVJs in *csm4*Δ cells during sporulation (**Fig. S6**, bottom panels), indicating that the bouquet gene *CSM4* is not required for the formation of NVJs.

Mps3 and telomere-led chromosomes are excluded from NVJs during meiotic prophase

The NPC and V-ATPase are excluded from NVJs in starved haploid cells.[23-25] Here, we report that, although they were not present at the NVJs, Nup49-GFP and Nup49-tdm2 localized around the NE and Vma2-tdm2 localized around the vacuolar membranes in the wild-type zygotes (**Fig. 6A and B**). These results readily explain why the NE (revealed by Nup49-GFP) is distorted during meiotic prophase,[7,9] because the NVJ is shaped like a flat dish. We also showed that GFP fused to Sec61, an essential component of the Sec61 polypeptide translocon complex in the ER, was not excluded from the NVCs (**Fig. 6C**). The Sec61-GFP protein was expressed from its native promoter by using a 2μ expression vector. The ER consists of a reticulum that underlies the plasma membrane (cortical ER) and a reticulum that is associated with the NE (nuclear ER).[40] The nuclear ER is continuous with the ONM. Sec61-GFP was found in both the cortical and nuclear ER (**Fig. 6C**).

Our results also indicated that Mps3-GFP was preferentially excluded from the NVJs in wild-type zygotes (**Fig. 6D**). In contrast, Mps3-GFP, like Nup49-tdm2, was detected all around the NE in the *nvj1*Δ zygotes (**Fig. 6E**). In addition, the Mps3-GFP dots underwent normal RPMs along the NE in the *nvj1*Δ zygotes, as were observed in wild-type cells (**Vids. S1–S4**). We conclude that the NVJs are responsible for the exclusion of Mps3, the NPC and V-ATPase from NVCs in wild-type meiotic cells but apparently do not affect RPMs.

We next assayed telomere clustering (bouquet formation) by imaging of Rap1-GFP signals in a single zygote.[5] Nuclei that were subjectively identified as bouquets showed a single prominent Rap1-GFP/telomere cluster (**Fig. 7A**). Bouquet formation frequency was slightly higher in the *nvj1*Δ zygotes (11.6%, n = 800) than in wild-type zygotes (9.9%, n = 800) (**Fig. 7B**). In addition, we found no telomere cluster at NVJs in the wild-type zygotes. In contrast, telomere clusters were found all around the NE, including the NVCs, in the *nvj1*Δ zygotes (**Fig. 7C**). These results indicate that NVJs, acting as a physical barrier for Mps3, have a negative role in regulating NE-tethered chromosome movement during meiotic prophase.

NVJs are not essential for budding yeast meiosis or sporulation

It was reported that the *nvj1*Δ mutant is similar to the wild-type with respect to vacuole number, vacuole inheritance, and sporulation.[23] In contrast, because Vac8 has additional functions in vacuole inheritance and protein targeting from the cytoplasm to the vacuole,[22] the *vac8*Δ mutant is defective in sporulation.[23] We found in the SK1 background, the wild-type zygotes resulted in 70% tetrads, 23% triads, and 7% dyads. The *vac8*Δ zygotes generated 7% tetrads, 31% triads, and 59% dyads (**Table 1**). The *nvj1*Δ zygotes also exhibited alternation in the number of spores (i.e., 27% tetrads, 44% triads, and 28% dyads). The results of our tetrad dissection analyses further revealed that the *nvj1*Δ zygotes produced as many viable spores (98%) as the wild-type cells did, whereas the *vac8*Δ zygotes generated only 91% viable spores (**Table 1**).

We next applied live-cell imaging to examine Vma2-tdm2 and Nup49-tdm2 in the mature spores of the *nvj1*Δ zygotes. We found that Nvj1 does not affect vacuole inheritance (**Fig. S7A**) or NE segregation (**Fig. S7B**). The *nvj1*Δ/*nvj1*Δ *FOB1-GFP*/*FOB1-GFP* zygotes produced tetrads with a single Fob1-GFP per spore (**Fig. S7A**). In contrast, the tetrads generated by the *nvj1*Δ/*nvj1*Δ *FOB1-GFP*/*FOB1* heterozygous strain had only 2 spores with Fob1-GFP (**Fig. S7B**). Strong Fob1-GFP signals were also detected in the ascus lumens of these 2 zygotes, which is consistent with previous reports that budding yeast eliminates nucleolar proteins (e.g., Fob1) during spore packing and then synthesizes new nucleolar proteins de novo during spore maturation.[33,41] We conclude that both Nvj1 and NVJs are not essential for spore viability, vacuole inheritance, NE segregation or nucleolus regeneration.

Loss of NVJ partly rescues abnormal sporulation of the *csm4*Δ mutant

RPMs and bouquet formation during meiotic mid-prophase may serve as stringency factors to eliminate unwanted inter-chromosomal associations during the homolog pairing process.[5,7,13] Thus, we next examined whether NVJs contribute to the meiotic defects observed in the *csm4*Δ mutant, which exhibits the slowest RPMs among various mutants of the bouquet genes *CSM4*, *NDJ1*, and *MPS3*.[42] We found that the *csm4*Δ *nvj1*Δ double zygotes produced 35% tetrads, 35% triads, and 27% dyads, whereas the *csm4*Δ zygotes resulted in 14% tetrads, 33% triads, and 49% dyads (**Table 1**). These results indicate that the additional *nvj1*Δ deletion in the *csm4*Δ zygotes reduced the number of dyads but not that of triads. In addition, the *csm4*Δ *nvj1*Δ zygotes generated slightly more tetrads with 4 viable spores (54%) than the *csm4*Δ zygotes (51%). Although the NE-tethered meiotic chromosomes in the *csm4*Δ *nvj1*Δ double mutant were defective with respect to their RPMs, they could explore a larger nuclear surface area due to the absence of NVJs. The wider distribution of NE-tethered chromosomes might reduce unwanted inter-chromosomal entanglements, as the *nvj1*Δ deletion partly restored the *csm4*Δ mutant.

Nvj1-GFP overexpression in wild-type zygotes results in moderate sporulation and chromosome disjunction defects

It was previously reported that total NVJ area is limited by *NVJ1*, not *VAC8*, and that the overexpression of Nvj1-GFP increases the NVJ area.[23] We therefore hypothesized that the overexpression of Nvj1-GFP (or together with Vac8) in wild-type zygotes would result in a meiotic phenotype that is similar to that of the bouquet mutants (i.e., *csm4*Δ) using a plasmid containing the P_{REDI} promoter. Red1, like Zip1, is a meiosis-specific structural component of the synaptonemal complex.[43] We first confirmed that Nvj1-GFP overexpression in the wild-type meiotic cells moderately increased the NVJ area (**Fig. 7D**). Consistent with our hypothesis, we found that Nvj1-GFP overexpression in the wild-type cells moderately decreased the bouquet formation frequency (**Fig. 7E**) and sporulation efficiency (**Table 1**), as well as resulting in more tetrads (9–11%) with 2 or less viable spores (**Table 1**).

Discussion

The current study reveals 4 novel characteristics of NVJs during meiosis. First, NVJs form before the onset of premeiotic DNA replication and are retained throughout most of the sporulation process. Second, zygotic NVJs undergo scission alongside the NE during the 2 rounds of meiotic nuclear division. New Nvj1 proteins are also synthesized de novo during late meiosis and/or during spore maturation. As a result, NVJs exist in all 4 mature spores. Third, NVJs function as diffusion barriers to exclude Mps3, the NPC and V-ATPase, but not the polypeptide translocon Sec61 complex from the ONM and nuclear ER. Accordingly, Mps3-tethered chromosomes and bouquet formation rarely occurs at NVJs during meiotic mid-prophase. Lastly, the negative role of NVJs in regulating Mps3/telomore-tethered chromosome movement contributes to the meiotic defects of the *csm4*Δ mutant. In addition, the increase in NVJ area resulting from the overexpression of Nvj1-GFP (or with Vac8) in wild-type zygotes produced a moderate bouquet mutant-like phenotype.

The results of our live-cell imaging experiments are consistent with previous reports that a large portion of zygotic NE and vacuolar materials are discharged into the ascus lumen, and that vacuolar materials (e.g., the Pep4 proteases) are nearly completely regenerated during spore maturation.[33,37,38] However, notably and contrary to results reported previously,[33] we found that the NEs of all 4 mature spores, rather than emerging from de novo synthesis, are mainly segregated from the zygotic NE. Our data revealed that as the vacuolar contact sites of the NE, a significant fraction of zygotic NVJs undergo scission alongside the zygotic NEs and

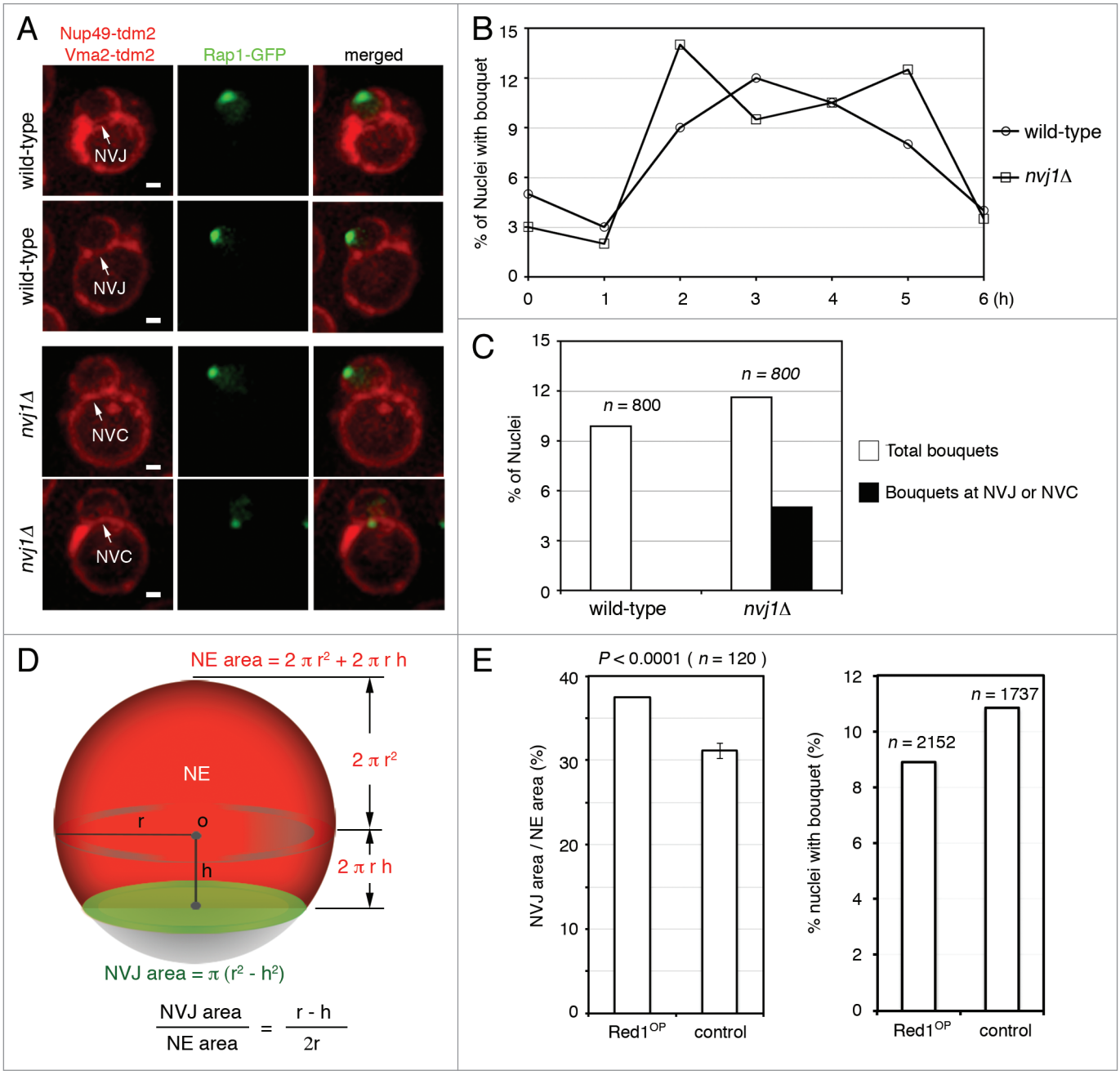

Figure 7. NVJs affect telomere clusters (bouquets). (**A**) NVJs exclude telomere clusters (bouquets). Representative images of telomere clusters or bouquets. For time-lapse imaging analyses of single, equatorial planes, 1 color image was taken every 0.33 s. For 3D reconstruction, Z-section images were captured of 30 slices spaced at 0.2 μm, or 14 slices at 0.6 μm in 1 s. Two-color, 3D, deconvolved, merged images of whole cells marked with a single prominent Rap1-GFP dot were scored as "bouquet." Bouquet formation rarely occurs at NVJs in wild-type cells, but was found over the entire nuclear envelope in *nvj1*Δ zygotes (bottom panel). (**B**) The *nvj1*Δ mutant is not defective in bouquet formation. Whole cells labeled and imaged as in (**A**) were assayed for bouquet formation, defined as a local maximum above a pre-defined threshold in the Rap1-GFP signal. (**C**) Wild-type and *nvj1*Δ samples of a given phenotype were taken at 2, 3, 4, and 5 h of sporulation and the data pooled and averaged. The total number of cells scored for each strain was 800. Open bar, percentage of nuclei showing a single prominent Rap1-GFP dot. Filled bars, percentage of nuclei showing a single prominent Rap1-GFP dot at the NVJ in wild-type zygotes or at the NVC in *nvj1*Δ zygotes. Scale bar: 1 μm. (**D**) Nvj1-GFP overexpression increased the NVJ area in wild-type cells during meiotic prophase. Method used to quantify the ratio of the NVJ area and the NE area. Mean values ± SEM (error bars) are shown from 120 meiotic cells (see Materials and Methods) (**E**) Nvj1-GFP overexpression decreased bouquet formation. Cells were imaged at 2, 3, 4, and 5 h of sporulation and the data pooled and averaged. The total number of cells scored for each strain was 2152 and 1737, respectively.

vacuolar membranes during the 2 rounds of meiotic division. As a result, NVJs frequently segregate together with the zygotic NE and vacuolar membranes into the mature spores.

Budding yeast vacuoles have several physiological functions including regulation of pH and osmosis, the hydrolysis of macromolecules, storage of amino acids, ions, polyphosphates, and

deleterious compounds.[44] Proteolysis is one of the best-known functions of the vacuole. Several vacuolar lumenal proteases have been known for many years, including Pep4/proteinase A, Prb1/proteinase B, and Prc1/carboxypeptidase Y.[45] The vacuole is also the final destination of cytoplasmic proteins and organelles delivered via macroautophagy, a ubiquitous process that occurs in all eukaryotic cells. These proteins or organelles are then degraded by vacuolar proteases. Importantly, autophagic proteins and vacuolar proteases are highly induced during budding yeast sporulation.[29,46] Mutation of autophagy-related genes (*ATG1* to *ATG10* and *ATG12*) leads to severe defects in sporulation.[44] The *pep4* mutant exhibits cell-cycle arrest before the first meiotic nuclear division and the *prb1* mutant sporulates poorly producing unusually small spores that remain embedded in a dense matrix.[29,47,48] In this report, we have demonstrated that the vacuole is continuously connected with the nucleus via NVJs during budding yeast meiosis. Intriguingly, NVJs are known to mediate PMN to degrade and recycle nuclear components.[21] The continuous connection between the nucleus and vacuoles via the NVJs, together with the indispensability of autophagic proteins and vacuolar proteases, indicate the need for a "cleaning" mechanism for the nucleus and/or chromosomes during sporulation. However, unlike the core autophagic proteins and vacuolar proteases, it seems that Nvj1 and Vac8 are not absolutely required for meiosis or sporulation. The roles of NVJ-independent macroautophagy and/or nucleophagy in meiosis require further investigation.

Finally, a potential implication of this study is that *nvj1*Δ mutant cells may be used to solve the technical difficulties found in isolating intact nuclei for the biochemical study of meiotic nuclear proteins because *nvj1*Δ nuclei are not physically associated with the vacuoles. Furthermore, the loss of NVJs as a result of the *nvj1*Δ deletion only slightly reduces the sporulation efficiency and does not significantly affect spore viability, vacuole inheritance, nucleolus regeneration, or NE segregation.

Table 1. Spore viability and sporulation efficiency

Strain	Ascus with 4, 3, 2, and 1 or 0 spores					
	4	3	2	1	0	n
wild type	70%	23%	7%	0%	0%	600
vac8Δ	7%	31%	59%	3%	0%	600
nvj1Δ	27%	44%	28%	1%	0%	600
csm4Δ	14%	33%	49%	4%	0%	600
csm4Δ nvj1Δ	35%	35%	27%	3%	0%	600
wild type mock P_{RED1} plasmid	47%	24%	23%	4%	2%	600
wild type P_{RED1}-*NVJ1-GFP* plasmid	38%	29%	27%	6%	0%	600
wild type P_{RED1}-*NVJ1-GFP* plasmid P_{RED1}-*VAC8* plasmid	16%	40%	32%	4%	8%	600
Strain	**Tetrads with 4, 3, 2, 1 or 0 viable spores**					**Overall viability**
	4	3	2	1	0	
wild type	91%	5%	4%	0%	0%	98% (n = 300)
vac8Δ	79%	13%	6%	1%	1%	92% (n = 300)
nvj1Δ	95%	4%	1%	0%	0%	98% (n = 300)
csm4Δ	51%	6%	22%	4%	17%	67% (n = 300)
csm4Δ nvj1Δ	54%	8%	17%	4%	17%	69% (n = 300)
wild type mock P_{RED1} plasmid	92%	6%	2%	0%	0%	98% (n = 512)
wild type P_{RED1}-*NVJ1-GFP* plasmid	81%	10%	5%	2%	2%	91% (n = 519)
wild type P_{RED1}-*NVJ1-GFP* plasmid P_{RED1}-*VAC8* plasmid	81%	8%	7%	2%	2%	91% (n = 521)

Materials and Methods

Yeast strains and sporulation cultures

All meiosis experiments were performed using diploid cells from isogenic SK1 strains. Yeast strains expressing fluorescent proteins were constructed as described previously.[31] Synchronous sporulation cultures were performed as described previously.[27,49]

Fluorescence microscopy

Yeast cells were attached to a slide coated with 200 μg/ml concanavalin A. Z-section images were captured by the DeltaVision system (Applied Precision) with a 100× objective lens (NA 1.4), a CoolSNAPTM HQ2 charge-coupled device camera (Photometrics) and filters for GFP (525 ± 25 nm), mCherry (632 ± 30 nm), CFP (470 ± 12 nm), DAPI (455 ± 25 nm), FITC (525 ± 18 nm), and TRITC (605 ± 26 nm). Deconvolution was processed using SoftWoRx, followed by 3D reconstruction with Imaris 7.0 (Bitplane). Images were processed using Photoshop (Adobe). For time-lapse imaging analyses of single, equatorial planes, one color image was taken every 0.33 s. For 3D reconstruction, Z-section images were captured for 30 slices spaced at 0.2 μm, or 14 slices spaced at 0.6 μm in 1 s.

Imaris software V.7.6.1 (Bitplane AG) was used to quantify relative Nvj1-GFP fluorescent intensity of the 4 mature spores in each tetrad. In short, for 3D reconstruction, Z section images were converted to the Imaris format and viewed in Surpass view.

After surface creation (based on fluorescence signals) intensity in each tetrad can be determined and compared as described in **Figure 2A**.

The NVJ area and the NE area in meiotic prophase cells were also determined by using Imaris software V.7.6.1 (Bitplane AG). Z section images were converted to Imaris format and viewed in Surpass model for 3D reconstruction. Surfaces of NE and NVJ were created by volumes occupied by the fluorescence signals. As described in **Figure 7D**, a sphere model was applied to determine the center (o) and the radius (r) of the nucleus. The distance between "o" and the NVJ surface was referred to as "h."

Statistical analyses were performed with the unpaired Student *t* test or by 2-way analysis of variance. Data are presented as mean ± SEM (standard errors), and *n* indicates the number of meiotic prophase cells analyzed in each experiment.

Electron microscopy

All electron microscopy procedures were performed at 4 °C or on ice. Cells were cultured in SPM and then prefixed with prefixation solution consisting of 2% glutaraldehyde in 0.1 M cacodylate buffer (0.1 M sodium cacodylate, pH 6.8), 1 mM $MgCl_2$, and 1 mM $CaCl_2$. After removal of the cell wall by zymolase, the cells were rinsed with 0.1 M cacodylate buffer, post-fixed in 0.5% osmium tetroxide and 0.8% potassium ferrocyanide, pre-stained with 1% uranyl acetate, dehydrated in a graded ethanol series, and embedded in Spurr resin. Ninety to 100 serial sections (each 75 nm in thickness) were cut, double-stained with 1% uranyl acetate and lead citrate, and then viewed on a Tecnai G2 Spirit TWIN transmission electron microscope (FEI Company) with a Gatan 794.10.BP2 MultiScan charge-coupled-device (CCD) camera.

Disclosure of Potential Conflicts of Interest

No potential conflicts of interest were disclosed.

Acknowledgments

This work was supported by grants to TFW from the National Science Council and Academia Sinica, Taiwan. We thank Sue-Ping Lee and Shu-Ping Tsai (IMB) for their help with the electron microscopy and fluorescence microscopy imaging, and Nancy Kleckner (Harvard University) for the Zip1(700)-GFP strain, Chao-Wen Wang (Institute of Plant and Microbial Biology, Academia Sinica) for providing the Sec61-GFP plasmid, and Miranda Loney (Agricultural Biotechnology Research Center, Academia Sinica) and Daniel J Klionsky (University of Michigan) for English editing.

Supplemental Materials

Supplemental materials may be found here:
www.landesbioscience.com/journals/autophagy/article/27192

References

1. Parvinen M, Söderström KO. Chromosome rotation and formation of synapsis. Nature 1976; 260:534-5; PMID:1264213; http://dx.doi.org/10.1038/260534a0
2. Ding DQ, Chikashige Y, Haraguchi T, Hiraoka Y. Oscillatory nuclear movement in fission yeast meiotic prophase is driven by astral microtubules, as revealed by continuous observation of chromosomes and microtubules in living cells. J Cell Sci 1998; 111:701-12; PMID:9471999
3. Scherthan H. Telomere attachment and clustering during meiosis. Cell Mol Life Sci 2007; 64:117-24; PMID:17219025; http://dx.doi.org/10.1007/s00018-006-6463-2
4. Conrad MN, Lee CY, Wilkerson JL, Dresser ME. *MPS3* mediates meiotic bouquet formation in *Saccharomyces cerevisiae*. Proc Natl Acad Sci U S A 2007; 104:8863-8; PMID:17495028; http://dx.doi.org/10.1073/pnas.0606165104
5. Conrad MN, Lee CY, Chao G, Shinohara M, Kosaka H, Shinohara A, Conchello JA, Dresser ME. Rapid telomere movement in meiotic prophase is promoted by *NDJ1, MPS3*, and *CSM4* and is modulated by recombination. Cell 2008; 133:1175-87; PMID:18585352; http://dx.doi.org/10.1016/j.cell.2008.04.047
6. Kosaka H, Shinohara M, Shinohara A. Csm4-dependent telomere movement on nuclear envelope promotes meiotic recombination. PLoS Genet 2008; 4:e1000196; PMID:18818742; http://dx.doi.org/10.1371/journal.pgen.1000196
7. Koszul R, Kim KP, Prentiss M, Kleckner N, Kameoka S. Meiotic chromosomes move by linkage to dynamic actin cables with transduction of force through the nuclear envelope. Cell 2008; 133:1188-201; PMID:18585353; http://dx.doi.org/10.1016/j.cell.2008.04.050
8. Wanat JJ, Kim KP, Koszul R, Zanders S, Weiner B, Kleckner N, Alani E. Csm4, in collaboration with Ndj1, mediates telomere-led chromosome dynamics and recombination during yeast meiosis. PLoS Genet 2008; 4:e1000188; PMID:18818741; http://dx.doi.org/10.1371/journal.pgen.1000188
9. Sonntag Brown M, Zanders S, Alani E. Sustained and rapid chromosome movements are critical for chromosome pairing and meiotic progression in budding yeast. Genetics 2011; 188:21-32; PMID:21339478; http://dx.doi.org/10.1534/genetics.110.125575
10. Bhalla N, Dernburg AF. Prelude to a division. Annu Rev Cell Dev Biol 2008; 24:397-424; PMID:18597662; http://dx.doi.org/10.1146/annurev.cellbio.23.090506.123245
11. Loidl J, Lukaszewicz A, Howard-Till RA, Koestler T. The *Tetrahymena* meiotic chromosome bouquet is organized by centromeres and promotes interhomolog recombination. J Cell Sci 2012; 125:5873-80; PMID:22976299; http://dx.doi.org/10.1242/jcs.112664
12. Wynne DJ, Rog O, Carlton PM, Dernburg AF. Dynein-dependent processive chromosome motions promote homologous pairing in *C. elegans* meiosis. J Cell Biol 2012; 196:47-64; PMID:22232701; http://dx.doi.org/10.1083/jcb.201106022
13. Koszul R, Kleckner N. Dynamic chromosome movements during meiosis: a way to eliminate unwanted connections? Trends Cell Biol 2009; 19:716-24; PMID:19854056; http://dx.doi.org/10.1016/j.tcb.2009.09.007
14. Chua PR, Roeder GS. Tam1, a telomere-associated meiotic protein, functions in chromosome synapsis and crossover interference. Genes Dev 1997; 11:1786-800; PMID:9242487; http://dx.doi.org/10.1101/gad.11.14.1786
15. Conrad MN, Dominguez AM, Dresser ME. Ndj1p, a meiotic telomere protein required for normal chromosome synapsis and segregation in yeast. Science 1997; 276:1252-5; PMID:9157883; http://dx.doi.org/10.1126/science.276.5316.1252
16. Trelles-Sticken E, Dresser ME, Scherthan H. Meiotic telomere protein Ndj1p is required for meiosis-specific telomere distribution, bouquet formation and efficient homologue pairing. J Cell Biol 2000; 151:95-106; PMID:11018056; http://dx.doi.org/10.1083/jcb.151.1.95
17. Jaspersen SL, Giddings TH Jr., Winey M. Mps3p is a novel component of the yeast spindle pole body that interacts with the yeast centrin homologue Cdc31p. J Cell Biol 2002; 159:945-56; PMID:12486115; http://dx.doi.org/10.1083/jcb.200208169
18. Beilharz T, Egan B, Silver PA, Hofmann K, Lithgow T. Bipartite signals mediate subcellular targeting of tail-anchored membrane proteins in *Saccharomyces cerevisiae*. J Biol Chem 2003; 278:8219-23; PMID:12514182; http://dx.doi.org/10.1074/jbc.M212725200
19. Burri L, Lithgow T. A complete set of SNAREs in yeast. Traffic 2004; 5:45-52; PMID:14675424; http://dx.doi.org/10.1046/j.1600-0854.2003.00151.x
20. Rabitsch KP, Tóth A, Gálová M, Schleiffer A, Schaffner G, Aigner E, Rupp C, Penkner AM, Moreno-Borchart AC, Primig M, et al. A screen for genes required for meiosis and spore formation based on whole-genome expression. Curr Biol 2001; 11:1001-9; PMID:11470404; http://dx.doi.org/10.1016/S0960-9822(01)00274-3
21. Kvam E, Goldfarb DS. Nucleus-vacuole junctions and piecemeal microautophagy of the nucleus in *S. cerevisiae*. Autophagy 2007; 3:85-92; PMID:17204844
22. Wang YX, Catlett NL, Weisman LS. Vac8p, a vacuolar protein with armadillo repeats, functions in both vacuole inheritance and protein targeting from the cytoplasm to vacuole. J Cell Biol 1998; 140:1063-74; PMID:9490720; http://dx.doi.org/10.1083/jcb.140.5.1063
23. Pan X, Roberts P, Chen Y, Kvam E, Shulga N, Huang K, Lemmon S, Goldfarb DS. Nucleus-vacuole junctions in *Saccharomyces cerevisiae* are formed through the direct interaction of Vac8p with Nvj1p. Mol Biol Cell 2000; 11:2445-57; PMID:10888680; http://dx.doi.org/10.1091/mbc.11.7.2445

24. Roberts P, Moshitch-Moshkovitz S, Kvam E, O'Toole E, Winey M, Goldfarb DS. Piecemeal microautophagy of nucleus in *Saccharomyces cerevisiae.* Mol Biol Cell 2003; 14:129-41; PMID:12529432; http://dx.doi.org/10.1091/mbc.E02-08-0483
25. Severs NJ, Jordan EG, Williamson DH. Nuclear pore absence from areas of close association between nucleus and vacuole in synchronous yeast cultures. J Ultrastruct Res 1976; 54:374-87; PMID:176417; http://dx.doi.org/10.1016/S0022-5320(76)80023-8
26. Dawaliby R, Mayer A. Microautophagy of the nucleus coincides with a vacuolar diffusion barrier at nuclear-vacuolar junctions. Mol Biol Cell 2010; 21:4173-83; PMID:20943953; http://dx.doi.org/10.1091/mbc.E09-09-0782
27. Lai YJ, Lin FM, Chuang MJ, Shen HJ, Wang TF. Genetic requirements and meiotic function of phosphorylation of the yeast axial element protein Red1. Mol Cell Biol 2011; 31:912-23; PMID:21173162; http://dx.doi.org/10.1128/MCB.00895-10
28. Lin FM, Lai YJ, Shen HJ, Cheng YH, Wang TF. Yeast axial-element protein, Red1, binds SUMO chains to promote meiotic interhomologue recombination and chromosome synapsis. EMBO J 2010; 29:586-96; PMID:19959993; http://dx.doi.org/10.1038/emboj.2009.362
29. Zubenko GS, Jones EW. Protein degradation, meiosis and sporulation in proteinase-deficient mutants of *Saccharomyces cerevisiae.* Genetics 1981; 97:45-64; PMID:7021321
30. Nelson H, Mandiyan S, Nelson N. A conserved gene encoding the 57-kDa subunit of the yeast vacuolar H+-ATPase. J Biol Chem 1989; 264:1775-8; PMID:2521486
31. Sheff MA, Thorn KS. Optimized cassettes for fluorescent protein tagging in *Saccharomyces cerevisiae.* Yeast 2004; 21:661-70; PMID:15197731; http://dx.doi.org/10.1002/yea.1130
32. Sym M, Engebrecht JA, Roeder GS. ZIP1 is a synaptonemal complex protein required for meiotic chromosome synapsis. Cell 1993; 72:365-78; PMID:7916652; http://dx.doi.org/10.1016/0092-8674(93)90114-6
33. Fuchs J, Loidl J. Behaviour of nucleolus organizing regions (NORs) and nucleoli during mitotic and meiotic divisions in budding yeast. Chromosome Res 2004; 12:427-38; PMID:15252239; http://dx.doi.org/10.1023/B:CHRO.0000034726.05374.db
34. Kobayashi T, Horiuchi T. A yeast gene product, Fob1 protein, required for both replication fork blocking and recombinational hotspot activities. Genes Cells 1996; 1:465-74; PMID:9078378; http://dx.doi.org/10.1046/j.1365-2443.1996.d01-256.x
35. Moreno-Borchart AC, Knop M. Prospore membrane formation: how budding yeast gets shaped in meiosis. Microbiol Res 2003; 158:83-90; PMID:12906380; http://dx.doi.org/10.1078/0944-5013-00194
36. Neiman AM. Sporulation in the budding yeast *Saccharomyces cerevisiae.* Genetics 2011; 189:737-65; PMID:22084423; http://dx.doi.org/10.1534/genetics.111.127126
37. Roeder AD, Shaw JM. Vacuole partitioning during meiotic division in yeast. Genetics 1996; 144:445-58; PMID:8889511
38. Suda Y, Nakanishi H, Mathieson EM, Neiman AM. Alternative modes of organellar segregation during sporulation in *Saccharomyces cerevisiae.* Eukaryot Cell 2007; 6:2009-17; PMID:17905927; http://dx.doi.org/10.1128/EC.00238-07
39. Clyne RK, Katis VL, Jessop L, Benjamin KR, Herskowitz I, Lichten M, Nasmyth K. Polo-like kinase Cdc5 promotes chiasmata formation and cosegregation of sister centromeres at meiosis I. Nat Cell Biol 2003; 5:480-5; PMID:12717442; http://dx.doi.org/10.1038/ncb977
40. Rose MD, Misra LM, Vogel JP. *KAR2*, a karyogamy gene, is the yeast homolog of the mammalian BiP/GRP78 gene. Cell 1989; 57:1211-21; PMID:2661018; http://dx.doi.org/10.1016/0092-8674(89)90058-5
41. Unal E, Kinde B, Amon A. Gametogenesis eliminates age-induced cellular damage and resets life span in yeast. Science 2011; 332:1554-7; PMID:21700873; http://dx.doi.org/10.1126/science.1204349
42. Lee CY, Conrad MN, Dresser ME. Meiotic chromosome pairing is promoted by telomere-led chromosome movements independent of bouquet formation. PLoS Genet 2012; 8:e1002730; PMID:22654677; http://dx.doi.org/10.1371/journal.pgen.1002730
43. Rockmill B, Roeder GS. *RED1*: a yeast gene required for the segregation of chromosomes during the reductional division of meiosis. Proc Natl Acad Sci U S A 1988; 85:6057-61; PMID:3413075; http://dx.doi.org/10.1073/pnas.85.16.6057
44. Klionsky DJ. The molecular machinery of autophagy: unanswered questions. J Cell Sci 2005; 118:7-18; PMID:15615779; http://dx.doi.org/10.1242/jcs.01620
45. Van Den Hazel HB, Kielland-Brandt MC, Winther JR. Review: biosynthesis and function of yeast vacuolar proteases. Yeast 1996; 12:1-16; PMID:8789256; http://dx.doi.org/10.1002/(SICI)1097-0061(199601)12:1<1::AID-YEA902>3.0.CO;2-N
46. Chu S, DeRisi J, Eisen M, Mulholland J, Botstein D, Brown PO, Herskowitz I. The transcriptional program of sporulation in budding yeast. Science 1998; 282:699-705; PMID:9784122; http://dx.doi.org/10.1126/science.282.5389.699
47. Betz H, Weiser U. Protein degradation during yeast sporulation. Enzyme and cytochrome patterns. Eur J Biochem 1976; 70:385-95; PMID:188644; http://dx.doi.org/10.1111/j.1432-1033.1976.tb11028.x
48. Zubenko GS, Park FJ, Jones EW. Genetic properties of mutations at the *PEP4* locus in *Saccharomyces cerevisiae.* Genetics 1982; 102:679-90; PMID:6764902
49. Cheng CH, Lo YH, Liang SS, Ti SC, Lin FM, Yeh CH, Huang HY, Wang TF. SUMO modifications control assembly of synaptonemal complex and polycomplex in meiosis of *Saccharomyces cerevisiae.* Genes Dev 2006; 20:2067-81; PMID:16847351; http://dx.doi.org/10.1101/gad.1430406